Inorganic Chemistry

Article

pubs.acs.org/IC

$Zn_2(VO_4)(IO_3)$: A Novel Polar Zinc(II) Vanadium(V) Iodate with a Large SHG Response

Bing-Ping Yang, Chun-Li Hu, Xiang Xu, Chao Huang, and Jiang-Gao Mao*

State Key Laboratory of Structural Chemistry, Fujian Institute of Research on the Structure of Matter, Chinese Academy of Sciences, Fuzhou 350002, People's Republic of China

Supporting Information

ABSTRACT: The synthesis, crystal and electronic structures, and optical properties of the first zinc(II) vanadium(V) iodate, namely, $Zn_2(VO_4)(IO_3)$, are reported. $Zn_2(VO_4)(IO_3)$ crystallizes in the noncentrosymmetric (NCS) and polar space group *Pc* (No. 7) with a = 5.2714(8) Å, b = 10.0402(11) Å, c = 5.5070(8) Å, β = 101.326(10)°, and Z = 2. It displays a novel three-dimensional (3D) network structure composed of ZnO_5, ZnO_6, VO_4, and IO_3 polyhedra. One-dimensional (1D) chains of edge-sharing ZnO_5 polyhedra and 1D chains of corner-sharing ZnO_6 octahedra along the *c*-axis are interconnected via corner-sharing into a two-dimensional (2D) zinc oxide layer, and such layers are bridged by both VO_4 tetrahedra and IO_3 groups into a 3D network. The polarity in the structure is imparted by the alignment of the stereochemically active lone pairs of the iodate anions along the *c*-axis. The second harmonics generation (SHG) measurements on powder samples of $Zn_2(VO_4)(IO_3)$ under 1064-nm laser radiation revealed a large response of ~6 × KDP, which is Type I phase-matchable. Thermal stability and optical properties, as well as theoretical calculations based on DFT methods, were also performed.

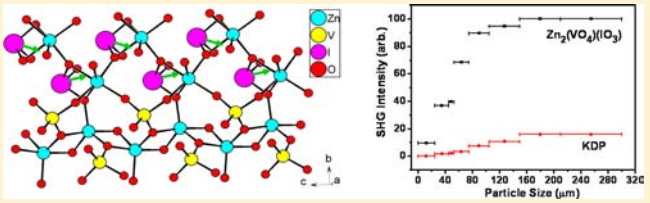

INTRODUCTION

The search of new second-order nonlinear optical (NLO) material is of current interest and great importance, because of their important applications in photonic technologies.[1] In the past decades, significant efforts have been made for the discoveries of new second-order NLO crystals, which have brought considerably useful NLO materials, such as β-BaB_2O_4 (BBO), LiB_3O_5 (LBO), KH_2PO_4 (KDP), $KTiOPO_4$ (KTP), $LiNbO_3$ (LN), $ZnGeP_2$, and $AgGaSe_2$.[2,3] On the basis of the structure–property relationships, the presence of the asymmetric or polar units are important for the formation of noncentrosymmetric (NCS) compounds with second-harmonic generation (SHG). As for the metal oxides, the known NLO active asymmetric units mainly include planar BO_3^{3-} groups,[4] second-order Jahn–Teller (SOJT) distorted d^0 transition metals (e.g., Mo^{6+}, V^{5+}, Ti^{4+}),[5] and lone-pair cations (e.g., I^{5+}, Se^{4+}, Bi^{3+}, Pb^{2+}).[6,7] The combination of two types of such asymmetric units into the same compound will enable an addition of their polarizations when those asymmetric building units are properly aligned, which has been demonstrated to be an effective strategy to design new NCS or polar materials with excellent SHG properties.[8−10]

In the 1970s, a number of ternary metal iodates have been prepared and their NLO, ferroelectric, piezoelectric, and pyroelectric properties have been studied.[11] During the past two decades, a series of metal iodates that contain SOJT distorted d^0 transition metals with excellent SHG properties have been synthesized in succession.[9,10] Recently, Halasyamani's group, as well as our group, found that the introduction of other lone-pair-containing cations such as lead(II) or bismuth(III) into the metal iodates can also afford materials with excellent SHG properties.[12] It is well-known that the Jahn–Teller distortion can occur not only in Cu^{2+} with partially filled *d*-orbitals but also in Zn^{2+} or Cd^{2+} with fully occupied *d*-orbitals.[13] Such examples include $ZnSnO_3$,[14] and $Zn_2(MoO_4)(AO_3)$ (A = Se^{4+} or Te^{4+}),[15] borates such as $Cd_4BiO(BO_3)_3$[16] and $Cd_4ReO(BO_3)_3$,[17] and $Na_3Cd_3B(PO_4)_4$,[18] all of which possess NCS or polar structures and exhibit large NLO coefficients. To the best of our knowledge, no metal iodates containing both d^{10}- and d^0-transition-metal ions has been reported, although several ternary or quaternary d^{10} transition-metal iodates have been reported,[19] among which $Zn(OH)(IO_3)$ and $K_2Zn(IO_3)_4(H_2O)_2$ are polar and exhibit moderate SHG responses.[19e] It is hoped that the cooperation effect of the above three types of asymmetrical units will lead to many new compounds with novel structures and good SHG properties. Based on this idea, the first zinc(II) vanadium(V) iodate, namely, $Zn_2(VO_4)(IO_3)$, with a large SHG response of ~6 × KDP (KH_2PO_4) (or ~240 × α-quartz) has been prepared and structurally characterized. Herein, we report its synthesis, crystal, and electronic structures, as well as optical properties.

EXPERIMENTAL SECTION

Materials and Methods. All of the chemicals were analytically pure from commercial sources and used without further purification. $Zn(CH_3COO)_2{\cdot}2H_2O$ (≥98%), V_2O_5 (≥99.9), and I_2O_5 (≥99%) were purchased from the Shanghai Reagent Factory. Microprobe elemental analyses were performed on a field-emission scanning

Received: February 7, 2013
Published: April 5, 2013

   dx.doi.org/10.1021/ic4003324 | *Inorg. Chem.* 2013, 52, 5378−5384

electron microscopy (FESEM) system (Model JSM6700F) equipped with an energy-dispersive X-ray spectroscopy (EDS) system (Oxford INCA). The powder X-ray diffraction (XRD) data were collected on a Model DMAX-2500 diffractometer using graphite-monochromated Cu Kα radiation in the 2θ range of 5°−65° with a step size of 0.05°. Thermogravimetric analysis (TGA) and differential scanning calorimetry (DSC) studies were all carried out with a Netzsch Model STA 449F3 instrument. The sample and reference (Al_2O_3) were enclosed in a platinum crucible and heated at a rate of 10 °C/min from room temperature to 1000 °C under a nitrogen atmosphere. The IR spectrum was recorded on a Magna 750 FT-IR spectrometer as KBr pellets in the range of 4000−450 cm^{-1}. The UV−vis absorption and optical diffuse reflectance spectra were measured at room temperature with a PE Lambda 900 UV−visible spectrophotometer in the range of 200−2500 nm. A $BaSO_4$ plate was used as a standard (100% reflectance). The absorption spectrum was calculated from reflectance spectrum using the Kubelka−Munk function:[20]

$$\frac{\alpha}{S} = \frac{(1-R)^2}{2R}$$

where α is the absorption coefficient, S the scattering coefficient (which is practically wavelength independent when the particle size is larger than 5 μm), and R the reflectance. The measurement of the powder frequency-doubling effect was carried out by means of the method of Kurtz and Perry.[21] The fundamental wavelength is 1064 nm generated by a Q-switched Nd:YAG laser. The SHG wavelength is 532 nm. KH_2PO_4 (KDP) was used as a reference to assume the effect. SHG efficiency has been shown to be dependent strongly on particle size; thus, samples of KDP and $Zn_2(VO_4)(IO_3)$ were ground and sieved into several distinct particle size ranges (0−25, 25−45, 45−53, 53−75, 75−105, 105−150, 150−210, and 210−300 μm). All of the samples were placed in separate capillary tubes. No index-matching fluid was used in any of the experiments.

Preparations of $Zn_2(VO_4)(IO_3)$. Single crystals of $Zn_2(VO_4)(IO_3)$ were synthesized by the hydrothermal reactions of a mixture of $Zn(CH_3COO)_2{\cdot}2H_2O$ (0.5 mmol, 110 mg), V_2O_5 (0.11 mmol, 20 mg), I_2O_5 (0.92 mmol, 310 mg), and 2 mL of water sealed in an autoclave equipped with a Teflon liner (23 mL) at 190 °C for 3 days, and then cooled to 50 °C at 3 °C/h. The final reaction product was washed with water and ethanol, and then dried in air. Colorless plate-shaped single crystals of $Zn_2(VO_4)(IO_3)$ were collected in a ca. 81% yield, based on V. The energy-dispersive spectrometry (EDS) elemental analyses on several single crystals of $Zn_2(VO_4)(IO_3)$ gave an average molar ratio of Zn/V/I of 1.8:1.0:1.1, which is in good agreement with that determined from single-crystal XRD studies.

Single-Crystal Structure Determination. A colorless, plate-shaped single crystal (dimensions of 0.2 mm × 0.2 mm × 0.05 mm) was glued on to a glass fiber and data were collected on a SCX mini CCD diffractometer equipped with graphite-monochromated Mo Kα radiation (λ = 0.71073 Å) at 293 K. The datasets were corrected for Lorentz and polarization factors, as well as for absorption, by a SADABS program.[22] The structure was solved by the direct method and refined by full-matrix least-squares fitting on F^2 by SHELX-98.[22] All atoms were refined with anisotropic thermal parameters. The Flack parameters were refined to 0.08(3), indicating the correctness of its absolute structure. The structure was checked for missing symmetry elements using PLATON.[23] Crystallographic data and structural refinements for the compound are summarized in Table 1. Important bond lengths are listed in Table 2. More details on the crystallographic studies, as well as atom displacement parameters, are given in the Supporting Information.

Theoretical Basis. Single-crystal data were used for the electronic and optical properties calculations. All calculations were carried out using the total-energy code of CASTEP.[24] The total energy was calculated within the framework of nonlocal gradient-corrected approximations [Perdew-Burke-Ernzerhof (PBE) functional].[25] The interactions between the ionic cores and the electrons was described by the norm-conserving pseudo-potential.[26] The following orbital electrons were treated as valence electrons: Zn $3d^{10}4s^2$, V $3d^34s^2$, I $5s^25p^5$, and O $2s^22p^4$. The number of plane waves included in the basis was determined by a cutoff energy of 600 eV, and the numerical integration of the Brillouin zone was performed using a 5 × 2 × 5 Monkhorst-Pack k-point sampling.

Table 1. Crystallographic Data for $Zn_2(VO_4)(IO_3)$

parameter	value
compound	$Zn_2(VO_4)(IO_3)$
formula	IO_7VZn_2
fw	420.58
temp, K	293(2)
space group	Pc (No. 7)
a, Å	5.2714(8)
b, Å	10.0402(11)
c, Å	5.5070(8)
β, deg	101.326(10)
V, Å^3	285.79(7)
Z	2
D_{calc}, g cm^{-3}	4.887
μ, mm^{-1}	15.310
Flack factor	0.08(3)
GOF	1.088
R1, wR2 [$I > 2\sigma(I)$]	0.0242, 0.0614
R1, wR2 (all data)	0.0245, 0.0614

[a] $R_1 = \sum||F_o| - |F_c||/\sum|F_o|$, $wR_2 = \{\sum w[(F_o)^2 - (F_c)^2]^2/\sum w[(F_o)^2]^2\}^{1/2}$.

Table 2. Selected Bond Lengths for $Zn_2(VO_4)(IO_3)$

bond pairing	bond length (Å)	bond pairing	bond length (Å)
Zn(1)−O(11)	1.977(6)	Zn(2)−O(1) #3	2.015(7)
Zn(1)−O(3) #1	2.012(7)	Zn(2)−O(13) #3	2.033(6)
Zn(1)−O(4)	2.016(6)	Zn(2)−O(12) #4	2.049(6)
Zn(1)−O(3)	2.082(6)	Zn(2)−O(11)	2.154(6)
Zn(1)−O(4) #1	2.133(6)	Zn(2)−O(12)	2.192(6)
V(1)−O(1)	1.656(7)	Zn(2)−O(2) #5	2.231(7)
V(1)−O(4) #6	1.716(6)	I(1)−O(13)	1.805(6)
V(1)−O(3)	1.725(6)	I(1)−O(11)	1.853(6)
V(1)−O(2)	1.761(7)	I(1)−O(12)	1.860(6)
		I(1)−O(2) #7	2.245(6)

[a] Symmetry transformations used to generate equivalent atoms: #1, x, $-y+1$, $z+{}^1/_2$; #2, x, $-y+1$, $z-{}^1/_2$; #3, $x+1$, y, z; #4, x, $-y+2$, $z-{}^1/_2$; #5, $x+1$, y, $z+1$; #6, $x-1$, $-y+1$, $z-{}^1/_2$; and #7, x, y, $z+1$.

The calculations of linear optical properties in terms of the complex dielectric function $\varepsilon(\omega) = \varepsilon_1(\omega) + i\varepsilon_2(\omega)$ were made. The imaginary part of the dielectric function (ε_2) was given in the following equation:[27]

$$\varepsilon_2^{ij}(\omega) = \frac{8\pi^2\hbar^2e^2}{m^2V}\sum_k\sum_{cv}(f_c - f_v)\frac{p_{cv}^i(k)p_{vc}^j(k)}{E_{vc}^2} \times \delta[E_c(k) - E_v(k) - \hbar\omega] \quad (1)$$

The f_c and f_v represent the Fermi distribution functions of the conduction and valence bands, respectively. The term $P_{cv}^i(k)$ denotes the momentum matrix element transition from the energy level c of the conduction band to the level v of the valence band at a certain k-point in the Brillouin zones and V is the volume of the unit cell. The m, e, and $\hbar$ are the electron mass, charge, and Plank's constant, respectively.

The second-order optical properties were calculated based on momentum-gauge formalism with the minimal-coupling interaction Hamiltonian and within the independent-particle approximation.[28] The imaginary part of the frequency-dependent second-order susceptibility $\chi^{(2)}(2\omega,\omega,\omega)$ is obtained from the electronic band

dx.doi.org/10.1021/ic4003324 | Inorg. Chem. 2013, 52, 5378−5384

structures by using the expressions already given elsewhere.[29] Then, use the Kramers–Kronig relations, as required by causality, to obtain the real part:

$$\chi'^{(2)}(-2\omega, \omega, \omega) = \frac{2}{\pi} P \int_0^\infty d\omega' \frac{\omega' \chi''^{(2)}(2\omega', \omega', \omega')}{\omega'^2 - \omega^2} \quad (2)$$

In the present study, the δ function in the expressions for $\chi^{(2)}(2\omega,\omega,\omega)$[29a–c] is approximated by a Gaussian function with $\Gamma = 0.2$ eV. Furthermore, to ensure that the real part calculated via Kramer–Kronig transformation (eq 2) is reliable, at least 150 empty bands were used in SHG calculation. In addition, DFT-GGA fails to correctly predict the CB energies; therefore, the CB energy should be corrected by adding a scissor operator. Meanwhile, the momentum matrix elements were also renormalized.[29a]

RESULTS AND DISCUSSION

Synthesis. The replacements of I_2O_5 by HIO_3 or H_5IO_6 as the source of iodate anion can also produce the title compound. Some purple-black platelike solids of I_2(s) were observed as a byproduct, which was probably from the self-oxidation–reduction reaction of the excess I_2O_5. These I_2 solids were removed by washing with ethanol.

Structural Description. $Zn_2(VO_4)(IO_3)$ represents the first metal iodate containing both d^{10} and d^0 transition-metal ions; it exhibits a three-dimensional network structure that is composed of ZnO_5, ZnO_6, VO_4, and IO_3 polyhedra (see Figure 1). There are two Zn atoms, one V atom, one I atom, and seven O atoms in the asymmetric unit of the title compound. Zn(1) is five-coordinated by one iodate oxygen and four oxo anions in a trigonal bipyramidal geometry, whereas Zn(2) is octahedrally coordinated by four O atoms from three iodate anions and two oxo anions. The Zn(1)–O and Zn(2)–O bond lengths are in the ranges of 1.977(6)–2.133(6) Å and 2.015(7)–2.231(7) Å, respectively (see Table 2). The V^{5+} cation is in a tetrahedral coordination geometry, with the V–O distance being in the range of 1.656(7)–1.761(7) Å. The iodine(V) atom is in a highly asymmetric IO_3E trigonal pyramidal geometry, where the lone-pair E occupies the pyramidal site and the I–O distances range from 1.805(6) Å to 1.860(6) Å. I(1) is also bonded to O(2), with a much longer bond length of 2.245(6) Å, which belongs to the medium intramolecular contacts class, according to the reference.[30a] Several metal iodates containing such types of IO_4 polyhedra have been previously reported.[7b,12c,30] These Zn–O, V–O, and I–O bond distances are similar to those reported in related compounds.[10,19]

The $Zn(1)O_5$ polyhedra share edges (O3–O4) to form a 1D zinc oxide chain along the *c*-direction, whereas neighboring $Zn(2)O_6$ octahedra are also interconnected into chains along the *c*-direction via corner-sharing (O12). These two types of chains are interconnected into Zn–O layers that are parallel to the *bc*-plane via sharing corners (Figure 1a). The Zn–O–Zn bond angles are in the range of 95.5(3)°–130.2(3)°. Such neighboring zinc oxide layers are further interconnected by bridging VO_4 and IO_3 groups into a complicated 3D network. Each IO_3 group is bridged to one $Zn(2)O_6$ octahedron via edge-sharing and two $Zn(2)O_6$ octahedra and one $Zn(1)O_5$ polyhedron via corner-sharing from one zinc oxide layer, and one $Zn(2)O_6$ octahedron via corner-sharing from another zinc oxide layer. The I–O–Zn bond angles are in the range of 99.9(3)°–129.2(3)°. Each VO_4 tetrahedron share corners with four $Zn(1)O_5$ polyhedra from a zinc oxide layer and two $Zn(2)O_6$ octahedra from another zinc oxide layer. The V–O–Zn bond angles are in the range of 125.0(4)°–159.3(4)°. Results of bond valence calculations indicate that Zn, V, and I atoms are in oxidation states of +2, +5, and +5, respectively.[31] The calculated total bond valences are 2.017, 2.041, 5.108, and 5.157 (with the weak I–O bond (2.245(6) Å) included) for Zn(1), Zn(2), V(1), and I(1), respectively.

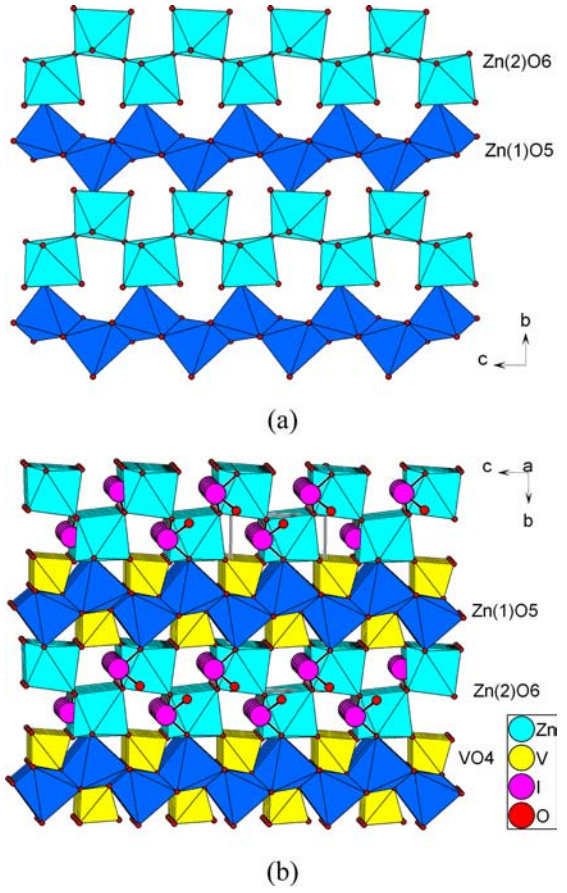

Figure 1. (a) Two-dimensional (2D) layer composed of the $Zn(1)O_5$ and $Zn(2)O_6$ polyhedra. (b) View of the 3D framework of $Zn_2(VO_4)(IO_3)$ down the *a*-axis. $Zn(1)O_5$ trigonal bipyramids, $Zn(2)O_6$ octahedra, and VO_4 tetrahedra are shaded in blue, turquoise, and yellow, respectively.

It is worthy to compare the structure of $Zn_2(VO_4)(IO_3)$ with those of the related zinc iodates. $Zn(IO_3)_2$ features a three-dimensional structure in which ZnO_6 octahedra share corners with six IO_3 polyhedra.[19b] (See Figure 2.) It is interesting to

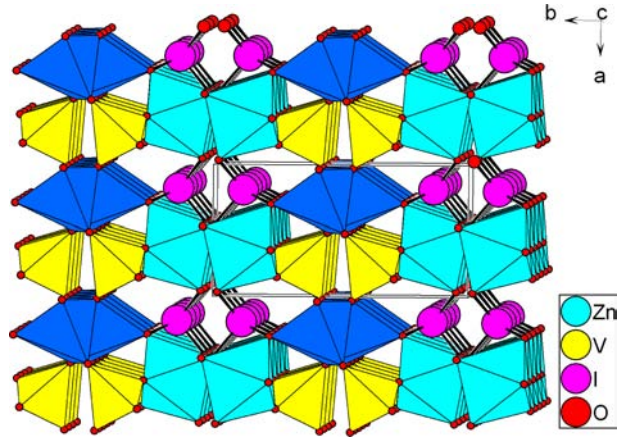

Figure 2. View of the structure of $Zn_2(VO_4)(IO_3)$ down the *c*-axis.

dx.doi.org/10.1021/ic4003324 | Inorg. Chem. 2013, 52, 5378–5384

note that $Zn(IO_3)(OH)$ features a layered structure composed of ZnO_6 and IO_3 groups, neighboring ZnO_6 octahedra share edges into a 1D chain along the *c*-axis, and the IO_3 groups serve as intrachain and interchain linkers.[19f] The alkali-metal vanadium(V) iodates mostly feature one-dimensional chains or two-dimensional layers anionic structure that are separated by alkali-metal cations.[10] The structure of the title compound is also comparable to that of $Zn_2(MoO_4)(SeO_3)$, in which ZnO_4 tetrahedra and ZnO_6 octahedra are interconnected via corner- and edge-sharing into a 1D zinc oxide chain, such chains are further bridged by MoO_4 and SeO_3 polyhedra into a layered architecture.[15] The vanadium(V) atoms in the previously reported metal iodates adopt either VO_5 or VO_6 coordination geometry and VO_4 tetrahedra found in $Zn_2(VO_4)(IO_3)$ is the first such example.

$Zn_2(VO_4)(IO_3)$ belongs to the polar space group *Pc* (No. 7), so it is relevant to discuss the structural origin of the polarity. The I^{5+} cations in the asymmetric unit are in an asymmetric coordination environment attributed to the VSEPR theory, being coordinated by three O atoms in a distorted trigonal-pyramidal geometry. Interestingly, the polarizations of all of the iodate groups are aligned along the *c*-axis to produce a large macroscopic dipole moment. A SOJT distortion is not possible for the tetrahedrally coordinated V^{5+} cation. The arrows in Figure 3a indicate the approximate direction of the local dipole moment on the IO_3 polyhedron. In a $Zn(2)O_6$ octahedron, the Zn(2)−O(1), Zn(2)−O(13), Zn(2)−O(12′) distances of 2.015(7), 2.033(6), and 2.049(6) Å are all shorter than those of Zn(2)−O(12), Zn(2)−O(11), Zn(2)−O(2) of 2.192(6), 2.154(6), and 2.231(7) Å, and the distortion of the $Zn(2)^{2+}$ cation is along the 3-fold rotational axis of the octahedron that passes through the triangle faces O1−O13−O12′ and O12−O11−O2, as shown in Figure 3b. The O(13)−Zn(2)−O(11) angle of 152° is significantly deviated from 180° for a perfect octahedron, which is due to the polar displacement of a d^{10} cation Zn^{2+}. The magnitude of the out-of-center distortion (Δd) was calculated to be a moderate value (0.51),[5] which is larger than the average magnitude of distortion for d^0 cations such as Ta^{5+} (0.38) and Ti^{4+} (0.34). The polar structure may be primarily characterized by IO_3 groups and a displacement of Zn from the center of octahedron.

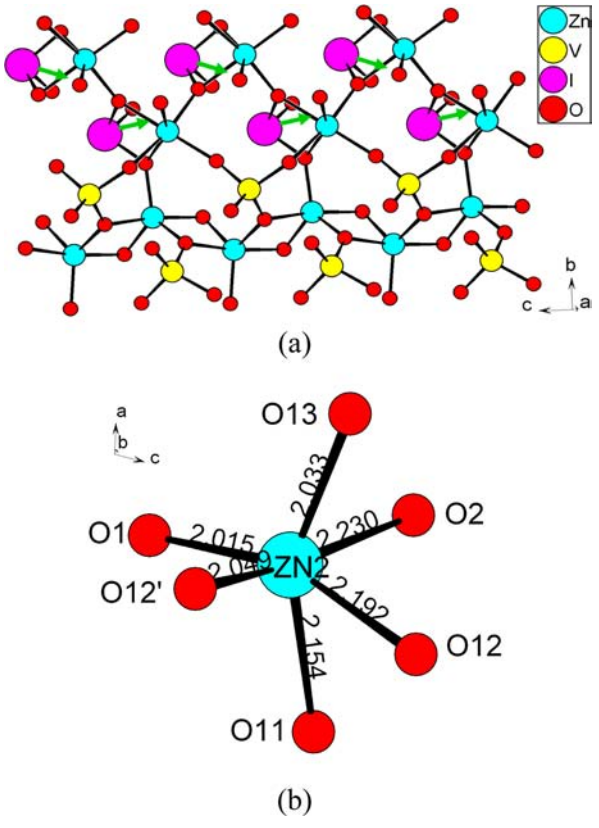

Figure 3. (a) View of the local structure of $Zn_2(VO_4)(IO_3)$ down the *a*-axis with the directions of the macroscopic polarities of the iodate groups indicated by small green arrows. (b) Coordination of oxygen atoms around the Zn(2) cation.

Thermal Stability Studies. Results of TGA studies indicate that $Zn_2(VO_4)(IO_3)$ is stable up to 530 °C. Upon further heating the iodate groups start to decompose through thermal disproportionation, which ends at 700 °C (Figure 4).

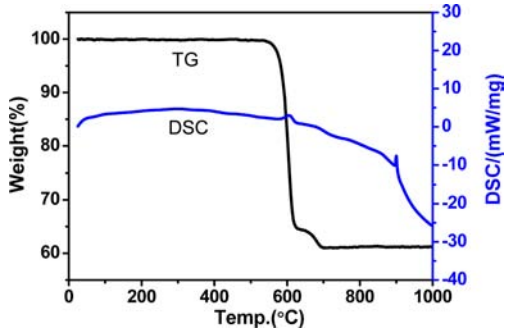

Figure 4. TGA and DSC diagrams for $Zn_2(VO_4)(IO_3)$.

These assignments are in agreement with the endothermic peaks at 604 °C in the DSC diagram (Figure 4). $Zn_2(VO_4)(IO_3)$ exhibits one weight loss step, which corresponds to the release of 0.5 molecules of I_2 and 1.25 molecules of O_2 per formula unit. The total weight loss of 38.9% at 600 °C is close to the calculated value of 39.6%.

Infrared and UV−vis Absorption and Diffuse Reflectance Spectra. Infrared (IR) spectrum indicate that $Zn_2(VO_4)(IO_3)$ is transparent in the range of 4000−1000 cm^{-1} (2.5−10 μm). IR spectrum shows the characteristic absorption bands of ν_{V-O} at 928 cm^{-1}. The symmetric ($\nu 1$) and antisymmetric ($\nu 3$) IO_3^- stretching bands appear in the range of 684−751 cm^{-1}, and the bands of its bending mode are observed at 475 cm^{-1} (see Figure S3 in the Supporting Information).[10,13] Its UV−vis absorption spectrum revealed little absorption from 0.4 μm to 2.5 μm (see Figure S4 in the Supporting Information). Hence, $Zn_2(VO_4)(IO_3)$ is transparent in the range of 0.4−10 μm, covering the visible (vis), near-infrared (NIR), and middle-infrared (IR) regions. Optical diffuse reflectance spectrum indicates an optical band gap of 3.26 eV; hence, $Zn_2(VO_4)(IO_3)$ is a wide-band-gap semiconductor (see Figure 5).

Nonlinear Optical Properties. The polar structure of $Zn_2(VO_4)(IO_3)$ prompts us to measure its SHG properties. Figure 6 shows the curves of the SHG signal intensity versus particle size for ground $Zn_2(VO_4)(IO_3)$ crystals. Features of the curves indicate that $Zn_2(VO_4)(IO_3)$ crystal belongs to the type I phase-matching class defined by Kurtz and Perry.[21] Comparison of the second-harmonic signal produced by the $Zn_2(VO_4)(IO_3)$ sample and the KDP sample in the same particle range from 150 to 210 μm reveals that $Zn_2(VO_4)(IO_3)$

dx.doi.org/10.1021/ic4003324 | Inorg. Chem. 2013, 52, 5378−5384

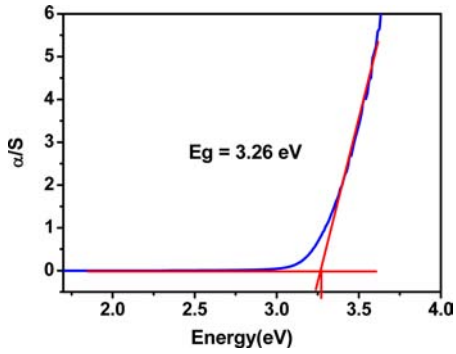

Figure 5. UV−vis diffuse reflectance spectrum for $Zn_2(VO_4)(IO_3)$.

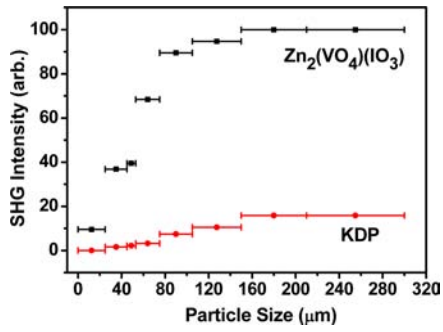

Figure 6. Particle size versus SHG intensity of $Zn_2(VO_4)(IO_3)$ and KDP.

exhibits a large SHG response of ~6 × KDP (~240 × α-quartz).

To better understand the magnitude and direction of the dipole moments, the local dipole moments for the IO_3, ZnO_6, ZnO_5 and VO_4 polyhedra and the net dipole moment within a unit cell for $Zn_2(VO_4)(IO_3)$ have been calculated using a method reported earlier.[32] With the lone-pair polyhedra, the lone pair is given a charge of −2 and is localized 1.23 Å from the I^{5+} cations.[33] The *x*-, *y*-, and *z*-components of the polarizations from two $I(1)O_3$ polyhedra in a unit cell are 2 × (6.04 D), (±5.44 D) and 2 × (14.87 D), respectively (D denotes Debye). Hence, the *x*-component of the polarizations coming from $I(1)O_3$ is relatively small, and the *y*-component of the polarizations from two $I(1)O_3$ polyhedra canceled out completely, while the *z*-component of their polarizations constructively adds to a value of 29.74 D. As for the other two $Zn(2)O_6$ polyhedra, two $Zn(1)O_5$ and two VO_4 polyhedra in a unit cell, the *y*-components of their polarizations canceled out completely, whereas those of the *x*-components and *z*-components have small values of 0.6−2.3 D (see Table S2 in the Supporting Information). The *x*-component and *z*-component net dipole moments for a unit cell are 13.1 and −27.5 D, respectively. Hence, the total net dipole moment for a unit cell is 30.51 D, and its direction is slightly deviated from the *c*-axis with an angle of 14.03° (see Figure S9 in the Supporting Information). Hence, the main contributions of the total polarizations come from the IO_3 groups, however the unique linking modes of $Zn(2)O_6$ and $Zn(1)O_5$ with the iodate groups are also helpful for the alignment of the lone pairs on the IO_3^- anions along the same direction to produce a macroscopic dipole moment that is approximately along the *c*-axis.

Theoretical Calculations. To gain further insights on the electronic structure and optical properties of $Zn_2(VO_4)(IO_3)$, theoretical calculations based on DFT methods were performed using the total-energy code CASTEP.[24]

The dispersions of energy bands are presented in Figure S5 in the Supporting Information and the density of states (DOS) is shown in Figure S6 in the Supporting Information. The top of valence bands (VB) is located at point A, and the bottom of conduction bands (CB) is located at point Y; hence, $Zn_2(VO_4)(IO_3)$ is an indirect-band-gap semiconductor (see Table S3 in the Supporting Information). The calculated band gap is 2.70 eV, which is smaller than the experimental value of 3.26 eV. This is not surprising, because it is well-known that the GGA does not accurately describe the eigenvalues of the electronic states, which often causes quantitative underestimation of band gaps for semiconductors and insulators.[34] Hence, during the subsequent optical property calculations, a scissor of 0.5 eV was adopted.

The bands can be assigned according to the total and partial density of states (DOS), as plotted in Figure S6 in the Supporting Information. From the DOS diagram, it is clear that the VB from −20.7 eV to −9.5 eV is mostly originated from O 2s and I 5s states, mixing with small amount of I 5p and O 2p states. Around the Fermi level, namely, −7.3−0 eV in VB and 2.3−6.5 eV in CB, O 2p, Zn 3d, I 5p, and V 3d states are all involved and overlapped fully among them, indicating the strong covalent interactions of Zn−O, I−O, and V−O bonds in the system.

Furthermore, we also explored the linear and nonlinear optical properties of the title polar crystal. It is noticeable that the calculated optical properties of the compound were based on its principal dielectric axis coordinate system. For the determination method of the principal dielectric axes of the monoclinic crystal, please see ref 10. The rotation angle θ between the original coordinate axes and the principal dielectric axes in the *ac*-plane was calculated to be 15.979° for $Zn_2(VO_4)(IO_3)$ crystal.

The linear optical response properties of $Zn_2(VO_4)(IO_3)$ were examined through calculating the complex dielectric function $\varepsilon(\omega) = \varepsilon_1(\omega) + i\varepsilon_2(\omega)$. Its imaginary part ($\varepsilon_2(\omega)$) can be used to describe the real transitions between the occupied and unoccupied electronic states. The imaginary and real parts of the frequency-dependent dielectric functions show obvious anisotropy along three dielectric axis directions (see Figures S7a and S7b in the Supporting Information). The curves of the averaged imaginary parts and real parts of the dielectric functions were obtained by $\varepsilon^{ave} = (\varepsilon_x + \varepsilon_y + \varepsilon_z)/3$ (see Figure S7c in the Supporting Information). The averaged imaginary part reveals the strongest adsorption peak at ~6.2 eV, which can be mainly assigned to the electronic interband transitions from the O 2p to V 3d and I 5p states. The average static dielectric constant $\varepsilon(0)$ is 5.08. The dispersion curves of refractive indices calculated by the formula $n^2(\omega) = \varepsilon(\omega)$ also display strong anisotropy and follow the order of $n^x > n^y > n^z$ in the low-energy range (see Figure S8 in the Supporting Information). The values of n^x, n^y, and n^z at 1064 nm (1.165 eV) are calculated to be 2.37, 2.31, and 2.19, respectively.

Based on the space group and the Kleinman symmetry, $Zn_2(VO_4)(IO_3)$ has six independent SHG tensors (d_{11}, d_{15}, d_{24}, d_{26}, d_{33}, and d_{35}). The frequency-dependent SHG tensors of $Zn_2(VO_4)(IO_3)$ are plotted in Figure 7. At the wavelength of 1064 nm (1.165 eV), the d_{11}, d_{15}, d_{24}, d_{26}, d_{33}, and d_{35} are 4.85 × 10^{-9}, 5.87 × 10^{-9}, 0.54 × 10^{-9}, 1.06 × 10^{-8}, 8.88 × 10^{-9}, and 1.79 × 10^{-8} esu, respectively. The calculated value of the highest SHG tensor (d_{35}) is much larger than our experimental

dx.doi.org/10.1021/ic4003324 | Inorg. Chem. 2013, 52, 5378−5384

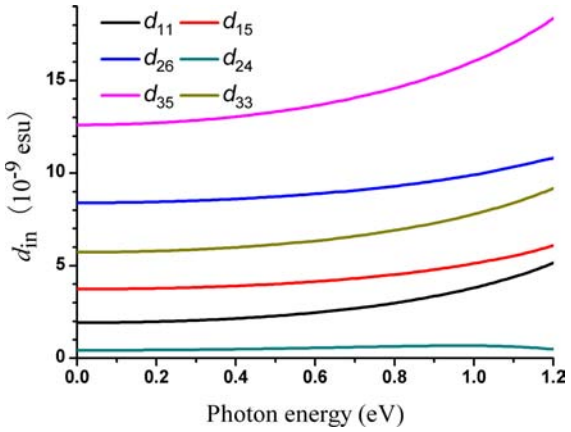

Figure 7. Calculated frequency-dependent SHG coefficients of $Zn_2(VO_4)(IO_3)$.

measurements on powder samples [6 × KDP (d_{36} = 1.1 × 10^{-9} esu)], because the calculations are based on single crystals that generate much stronger SHG coefficients.

CONCLUSIONS

In summary, the first iodate containing both d^0 and d^{10} transition metals, namely, $Zn_2(VO_4)(IO_3)$, has been prepared and structurally characterized. It features a complicated three-dimensional network structure composed of IO_3 groups, ZnO_6 octahedra, ZnO_5 trigonal bipyramids, and VO_4 tetrahedra. Moreover, it is the first member of the d^{10} transition metal−d^0 transition metal−iodate systems. The polarizations of all of the iodate groups are aligned along the *c*-axis to produce a large macroscopic dipole moment. From the second-harmonic generation (SHG) measurements on powders, $Zn_2(VO_4)(IO_3)$ is established to belong to Type I phase-matchable class with a large SHG response of ~6 × KH_2PO_4 (KDP), which is smaller than the results obtained from the theoretical calculations, because the calculations are based on single crystals that generate much larger SHG coefficients. It also has wide transparent region and high thermal stability. Based on these arguments, this compound is potentially a new candidate for applications as new second-order nonlinear optical (NLO) materials. Our future research efforts will be devoted to the growth of the large single crystals of $Zn_2(VO_4)(IO_3)$ and further study its optical properties such as refractive index, the Sellmeier equations, second-order NLO coefficients, and laser damage threshold.

ASSOCIATED CONTENT

Supporting Information

X-ray crystallographic file in CIF format, simulated and experimental powder X-ray diffraction patterns, and infrared and UV−vis absorption spectra for the compound. This material is available free of charge via the Internet at http://pubs.acs.org.

AUTHOR INFORMATION

Corresponding Author

*Fax: (+86)591-83714946. E-mail: mjg@fjirsm.ac.cn.

Notes

The authors declare no competing financial interest.

ACKNOWLEDGMENTS

We thank the National Natural Science Foundation of China (Nos. 21003127, 21231006, and 21203197) for their financial support.

REFERENCES

(1) (a) Chen, C.; Liu, G. *Annu. Rev. Mater. Sci.* **1986**, *16*, 203. (b) Wickleder, M. S. *Chem. Rev.* **2002**, *102*, 2011. (c) Ok, K. M.; Halasyamani, P. S. *Chem. Soc. Rev.* **2006**, *35*, 710 and references cited therein.

(2) (a) Becker, P. *Adv. Mater.* **1998**, *10*, 979. (b) Chen, C. T.; Wang, Y. B.; Wu, B. C.; Wu, K. C.; Zeng, W. L.; Yu, L. H. *Nature* **1995**, *373*, 322. (c) Chen, C. T.; Wu, B. C.; Jiang, A. D.; You, G. M. *Sci. Sin., Ser. B* **1984**, *14*, 598. (d) Hagerman, M. E.; Poeppelmeier, K. R. *Chem. Mater.* **1995**, *7*, 602. (e) Ballman, A. A.; Brown, H. *J. Cryst. Growth* **1967**, *1*, 311.

(3) (a) Dmitriev, V. G.; Gurzadyan, G. G.; Nikogosyan, D. N. *Handbook of Nonlinear Optical Crystals*; Springer: Berlin, 1991. (b) Boyd, G. D.; Buehler, E.; Storz, F. G. *Appl. Phys. Lett.* **1971**, *18*, 301. (c) Liao, J. H.; Marking, G. M.; Hsu, K. F.; Matsushita, Y.; Ewbank, M. D.; Borwick, R.; Cunningham, P.; Rosker, M. J.; Kanatzidis, M. G. *J. Am. Chem. Soc.* **2003**, *125*, 9484. (d) Zhang, Q.; Chung, I.; Jang, J. I.; Ketterson, J. B.; Kanatzidis, M. G. *J. Am. Chem. Soc.* **2009**, *131*, 9896.

(4) (a) Pan, S. L.; Smit, J. P.; Watkins, B.; Marvel, M. R.; Stern, C. L.; Poeppelmeier, K. R. *J. Am. Chem. Soc.* **2006**, *128*, 11631. (b) Wang, S. C.; Ye, N.; Li, W.; Zhao, D. *J. Am. Chem. Soc.* **2010**, *132*, 8779. (c) Huang, Y. Z.; Wu, L. M.; Wu, X. T.; Li, L. H.; Chen, L.; Zhang, Y. F. *J. Am. Chem. Soc.* **2010**, *132*, 12788. (d) Wu, H. P.; Pan, S. L.; Poeppelmeier, K. R.; Li, H. Y.; Jia, D. Z.; Chen, Z. H.; Fan, X. Y.; Yang, Y.; Rondinelli, J. M.; Luo, H. S. *J. Am. Chem. Soc.* **2011**, *133*, 7786.

(5) Halasyamani, P. S. *Chem. Mater.* **2004**, *16*, 3586 and references cited therein.

(6) Kim, S. H.; Yeon, J.; Halasyamani, P. S. *Chem. Mater.* **2009**, *21*, 5335.

(7) (a) Ok, K. M.; Halasyamani, P. S. *Angew. Chem., Int. Ed.* **2004**, *43*, 5489. (b) Phanon, D.; Gautier-Luneau, I. *Angew. Chem., Int. Ed.* **2007**, *46*, 8488. (c) Phanon, D.; Gautier-Luneau, I. *J. Mater. Chem.* **2007**, *17*, 1123. (d) Sun, C. F.; Hu, C. L.; Xu, X.; Mao, J. G. *Inorg. Chem.* **2010**, *49*, 9581.

(8) (a) Ra, H.-S.; Ok, K.-M.; Halasyamani, P. S. *J. Am. Chem. Soc.* **2003**, *125*, 7764. (b) Chi, E. O.; Ok, K. M.; Porter, Y.; Halasyamani, P. S. *Chem. Mater.* **2006**, *18*, 2070. (c) Kim, J. H.; Baek, J.; Halasyamani, P. S. *Chem. Mater.* **2007**, *19*, 5637. (d) Kong, F.; Huang, S.-P.; Sun, Z.-M.; Mao, J.-G.; Cheng, W.-D. *J. Am. Chem. Soc.* **2006**, *128*, 7750. (e) Jiang, H. L.; Huang, S. P.; Fan, Y.; Mao, J. G.; Cheng, W. D. *Chem.−Eur. J.* **2008**, *14*, 1972. (f) Mao, J. G.; Jiang, H. L.; Kong, F. *Inorg. Chem.* **2008**, *47*, 8498. (g) Zhou, Y.; Hu, C. L.; Hu, T.; Kong, F.; Mao, J. G. *Dalton Trans.* **2009**, 5747.

(9) (a) Sykora, R. E.; Ok, K. M.; Halasyamani, P. S.; Albrecht-Schmitt, T. E. *J. Am. Chem. Soc.* **2002**, *124*, 1951. (b) Shehee, T. C.; Sykora, R. E.; Ok, K. M.; Halasyamani, P. S.; Albrecht-Schmitt, T. E. *Inorg. Chem.* **2003**, *42*, 457. (c) Chang, H.-Y.; Kim, S.-H.; Halasyamani, P. S.; Ok, K. M. *J. Am. Chem. Soc.* **2009**, *131*, 2426. (d) Chang, H.-Y.; Kim, S.-H.; Ok, K. M.; Halasyamani, P. S. *J. Am. Chem. Soc.* **2009**, *131*, 6865. (e) Sun, C. F.; Hu, C. L.; Xu, X.; Ling, J. B.; Hu, T.; Kong, F.; Long, X. F.; Mao, J. G. *J. Am. Chem. Soc.* **2009**, *131*, 9486.

(10) (a) Sykora, R. E.; Ok, K. M.; Halasyamani, P. S.; Wells, D. M.; Albrecht-Schmitt, T. E. *Chem. Mater.* **2002**, *14*, 2741. (b) Yang, B. P.; Hu, C. L.; Xu, X.; Sun, C. F.; Zhang, J. H.; Mao, J. G. *Chem. Mater.* **2010**, *22*, 1545. (c) Sun, C. F.; Hu, C. L.; Xu, X.; Yang, B. P.; Mao, J. G. *J. Am. Chem. Soc.* **2011**, *133*, 5561. (d) Sun, C. F.; Yang, B. P.; Mao, J. G. *Sci. China: Chem.* **2011**, *54*, 911. (e) Chen, X. A.; Zhang, L.; Chang, X. A.; Zang, H. G.; Xiao, W. Q. *Acta Crystallogr., Sect. C: Cryst. Struct. Commun.* **2006**, *C62*, i76.

(11) (a) Abrahams, S. C.; Bernstein, J. L.; Elemans, J. B. A.; Verschoor, G. C. *J. Chem. Phys.* **1973**, *59*, 2007. (b) Abrahams, S. C.;

Sherwood, R. C.; Bernstein, J. L.; Nassau, K. *J. Solid State Chem.* **1973**, *7*, 205. (c) Nassau, K.; Cooper, A. S.; Shiever, J. W.; Prescott, B. E. *J. Solid State Chem.* **1973**, *8*, 260. (d) Liminga, R.; Abrahams, S. C. *Acta Crystallogr., Sect. A: Cryst. Phys., Diffr., Theor. Gen. Crystallogr.* **1975**, *31*, S81. (e) Abrahams, S. C.; Bernstein, J. L.; Nassau, K. *Solid State Commun.* **1976**, *18*, 1279. (f) Meschede, W.; Mattes, R. *Z. Anorg. Allg. Chem.* **1976**, *420*, 25.

(12) (a) Hu, T.; Qin, L.; Kong, F.; Zhou, Y.; Mao, J. G. *Inorg. Chem.* **2009**, *48*, 2193. (b) Nguyen, S. D.; Yeon, J.; Kim, S. H.; Halasyamani, P. S. *J. Am. Chem. Soc.* **2011**, *133*, 12422. (c) Cao, Z. B.; Yue, Y. C.; Yao, J. Y.; Lin, Z. S.; He, R.; Hu, Z. G. *Inorg. Chem.* **2011**, *50*, 12818. (d) Sun, C. F.; Hu, C. L.; Mao, J. G. *Chem. Commun.* **2012**, *48*, 4220.

(13) Wang, L. G.; Shi, W.; Yao, P.; Ni, Z. M.; Li, Y.; Liu, J. *Acta Phys.—Chim. Sin.* **2012**, *28*, 58.

(14) Inaguma, Y.; Yoshida, M.; Katsumata, T. *J. Am. Chem. Soc.* **2008**, *130*, 6704.

(15) Nguyen, S. D.; Kim, S. H.; Halasyamani, P. S. *Inorg. Chem.* **2011**, *50*, 5215.

(16) Zhang, W. L.; Cheng, W. D.; Zhang, H.; Geng, L.; Lin, C. S.; He, Z. Z. *J. Am. Chem. Soc.* **2010**, *132*, 1508.

(17) Zou, G.; Ma, Z.; Wu, K.; Ye, N. *J. Mater. Chem.* **2012**, *22*, 19911.

(18) Shi, Y.; Pan, S.; Dong, X.; Wang, Y.; Zhang, M.; Zhang, F.; Zhou, Z. *Inorg. Chem.* **2012**, *51*, 10870.

(19) (a) Phanon, D.; Bentria, B.; Jeanneau, E.; Benbertal, D.; Mosset, A.; Gautier-Luneau, I. *Z. Kristallogr.* **2006**, *221*, 635. (b) Liang, J.-K.; Wang, C.-G. *Acta Chim. Sin.* **1982**, *40*, 985. (c) Zloczysti, S.; Hartl, H.; Frydrych, R. *Acta Crystallogr., Sect. B: Struct. Crystallogr. Cryst. Chem.* **1976**, *32*, 753. (d) Bentria, B.; Benbertal, D.; Hebboul, Z.; Bagieu-Beucher, M.; Mosset, A. *Z. Anorg. Allg. Chem.* **2005**, *631*, 894. (e) Li, P.-X.; Hu, C.-L.; Xu, X.; Wang, R.-Y.; Sun, C.-F.; Mao, J.-G. *Inorg. Chem.* **2010**, *49*, 4599. (f) Lee, D. W.; Kim, S. B.; Ok, K. M. *Dalton Trans.* **2012**, *41*, 8348. (g) Peter, S.; Pracht, G.; Lange, N.; Lutz, H. D. *Z. Anorg. Allg. Chem.* **2000**, *626*, 208.

(20) Kubelka, P.; Munk, F. *Z. Tech. Phys.* **1931**, *12*, 593.

(21) Kurtz, S. K.; Perry, T. T. *J. Appl. Phys.* **1968**, *39*, 3798.

(22) Sheldrick, G. M. *SHELXTL, Crystallographic Software Package, Version 5.1*; Bruker-AXS: Madison, WI, 1998.

(23) Spek, A. L. *PLATON*; Utrecht University: Utrecht, The Netherlands, 2001.

(24) (a) Segall, M. D.; Lindan, P. L. D.; Probert, M. J.; Pickard, C. J.; Hasnip, P. J.; Clark, S. J.; Payne, M. C. *J. Phys.: Condens. Matter* **2002**, *14*, 2717. (b) Milman, V.; Winkler, B.; White, J. A.; Pickard, C. J.; Payne, M. C.; Akhmatskaya, E. V.; Nobes, R. H. *Int. J. Quantum Chem.* **2000**, *77*, 895.

(25) Perdew, J. P.; Burke, K.; Ernzerhof, M. *Phys. Rev. Lett.* **1996**, *77*, 3865.

(26) Lin, J. S.; Qteish, A.; Payne, M. C.; Heine, V. *Phys. Rev. B* **1993**, *B47*, 4174.

(27) Bassani, F.; Parravicini, G. P. *Electronic States and Optical Transitions in Solids*; Pergamon Press, Ltd.: Oxford, U.K., 1975; pp 149−154.

(28) (a) Ghahramani, E.; Moss, D. J.; Sipe, J. E. *Phys. Rev. B* **1991**, *43*, 8990. (b) Ghahramani, E.; Moss, D. J.; Sipe, J. E. *Phys. Rev. Lett.* **1990**, *64*, 2815.

(29) (a) Duan, C. G.; Li, J.; Gu, Z. Q.; Wang, D. S. *Phys. Rev. B* **1999**, *60*, 9435. (b) Guo, G. Y.; Chu, K. C.; Wang, D. S.; Duan, C. G. *Phys. Rev. B* **2004**, *69*, 205416. (c) Guo, G. Y.; Lin, J. C. *Phys. Rev. B* **2005**, *72*, 075416. (d) Guo, G. Y.; Lin, J. C. *Phys. Rev. B* **2008**, *77*, 049901.

(30) (a) Gautier-Luneau, I.; Suffren, Y.; Jamet, H.; Pilmé, J. *Z. Anorg. Allg. Chem.* **2010**, *636*, 1368. (b) Ok, K. M.; Halasyamani, P. S. *Inorg. Chem.* **2005**, *44*, 9353. (c) Bean, A. C.; Campana, C. F.; Kwon, O.; Albrecht-Schmitt, T. E. *J. Am. Chem. Soc.* **2001**, *123*, 8806. (d) Sykora, R. E.; Wells, D. M.; Albrecht-Schmitt, T. E. *Inorg. Chem.* **2002**, *41*, 2697.

(31) (a) Brown, I. D.; Altermatt, D. *Acta Crystallogr., Sect. B: Struct. Sci.* **1985**, *B41*, 244. (b) Brese, N. E.; O'Keeffe, M. *Acta Crystallogr., Sect. B: Struct. Sci.* **1991**, *B47*, 192.

(32) (a) Maggard, P. A.; Nault, T. S.; Stern, C. L.; Poeppelmeier, K. R. *J. Solid State Chem.* **2003**, *175*, 27. (b) Izumi, H. K.; Kirsch, J. E.; Stren, C. L.; Poeppelmeier, K. R. *Inorg. Chem.* **2005**, *44*, 884. (c) Sivakumar, T.; Chang, H. Y.; Baek, J.; Halasyamani, P. S. *Chem. Mater.* **2007**, *19*, 4710. (d) Chang, H. Y.; Kim, S. H.; Ok, K. M.; Halasyamani, P. S. *Chem. Mater.* **2009**, *21*, 1654.

(33) Galy, J.; Meunier, G.; Andersson, S.; Åström, A. *J. Solid State Chem.* **1975**, *13*, 142.

(34) (a) Okoye, C. M. I. *J. Phys.: Condens. Matter* **2003**, *15*, 5945. (b) Huang, S. P.; Cheng, W. D.; Wu, D. S.; Li, X. D.; Lan, Y. Z.; Li, F. F.; Shen, J.; Zhang, H.; Gong, Y. J. *J. Appl. Phys.* **2006**, *99*, Article No. 013516.